Analysis of Various Clutter Suppression Methods for a Ground-Based L-Band ARSR-3 Air Traffic Control Radar System

John Hodge

May 15th, 2014

Virginia Tech

ECE 5636: Radar Signal Processing

Final Exam Report

I. Abstract

In this project, an ARSE-3 ground based L-band, MTI radar used for civilian purposes in being considered. A patch of very radar reflective wooded hills is providing a significant amount RCS return preventing the radar system from picking up the target without using signal processing techniques. Obstacles, such as the wooded hills are referred to as clutter. In particular, this study focuses on stationary or very slow moving ground based clutter that will return a very low Doppler frequency.

In this analysis, the amount of ground clutter will be calculated along with the necessary levels of clutter attenuation. Clutter suppression techniques for MTI radar will be analyzed and simulated using the N-pulse delay line canceller. Similarly, an alternative method of clutter suppression known as Pulse Doppler Processing will also analyzed and simulated. Pulse Doppler Processing realizes the matched filter using the discrete Fourier transform to implemented digital filter banks. This work includes an analysis of how windowing techniques can be used to improve performance of a digital filter. From this work a good understanding of the problems presented by ground-based should be gained along with effective methods to suppress large amounts of clutter for radar detection purposes.

Table of Contents

II. Introduction

To begin Table 1.1 lists the necessary parameters and requirements needed to analyze this ARSR-3 radar system. For spacing saving purposes, most of the relevant introductory material was covered in the Abstract and is summarized again in the Conclusion. More relevant equations are stated in the analysis sections as they are relevant.

Operational Frequency	f = 1.3GHz
Transmission Wavelength	λ = 0.321m
Azimuthal Beamwidth	θ_{az} = 1.25° = 0.0218 radians
Pulse Width	τ = 2μs
PRF	f_p = 400Hz
Ground Clutter (Wooded Hills) Cross-Section Per Unit Area	$\sigma°$ = -20dB per m^2
Standard Deviation of Zero-Mean Gaussian Clutter Distribution	σ_v = 1.16 km/hr = 0.322 m/s → σ_c = 2.79Hz; Normalized: σ_f = 2.79Hz/400Hz = 6.98e-3; σ_ω = (2π)(σ_f) = (2π)(6.98e-3) = 0.0438 rad/s
Target RCS	σ_{target} = $2m^2$ = $3dBm^2$
Target Range	30 nmi = 34.5 miles = 55.56 km
Range of Anticipated Target Doppler Frequencies	50 Hz to 350 Hz
Anticipated Target Velocities	
Required Signal to Clutter Ratio (S/C)	15dB

Table 1: Summary of Relevant System Parameters and Requirements

For this system with a PRF = 400Hz, the unambiguous range of this radar is

$$R_{ua} = c/(2*PRF) = c/(2*400Hz) = 375km. \tag{2.1}$$

The Doppler frequency of the first blind speed, defined by the first null of the moving target indication (MTI) filter, occurs at F = PRF = 400Hz. Since the Doppler frequency of the first null is greater than the anticipated Doppler frequency shifts of 50Hz to 350Hz, range ambiguity can be ignored for the rest of this analysis. It will be assumed that the Doppler shift of received signals from credible targets will be < PRF = 400Hz. For this reason, N-pulse canceller designs will not need to be staggered.

N-pulse Canceller:

Two-Pulse Canceller:

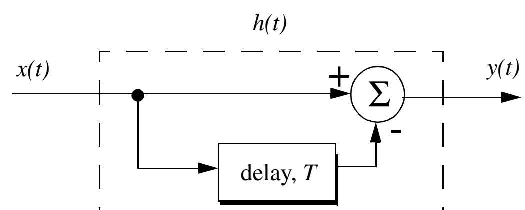

$$|H(f)|^2 = 4\left(\sin\left(\frac{\pi f}{f_r}\right)\right)^2$$

Three-Pulse Canceller:

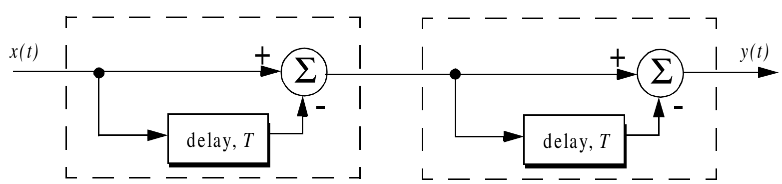

$$H(z) = (1 - z^{-1})^2 = 1 - 2z^{-1} + z^{-2}$$

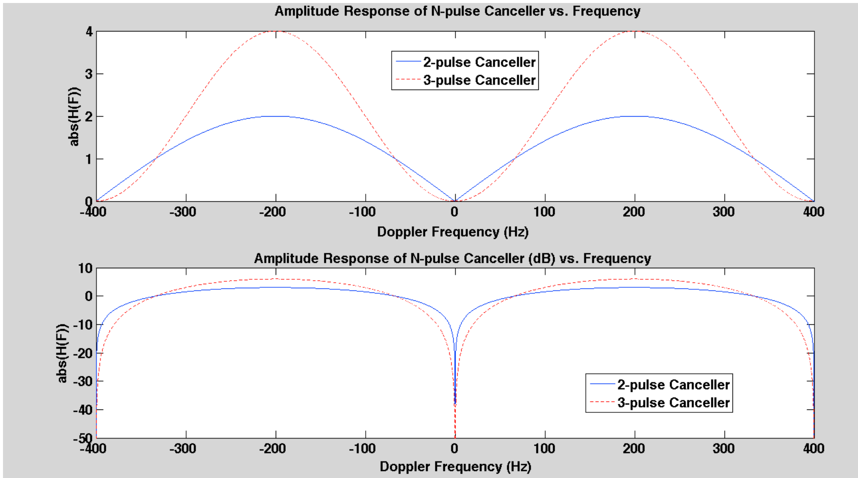

Figure 1: Frequency Spectrum Response on the Two and Three Pulse Canceller

III. Design and Analysis

Objective A: Show that clutter attenuation must be at least 47.6dB

The Doppler frequency of a target can be calculated from

$$f_d = \frac{2v_r}{\lambda} \tag{3.1}$$

where f_d is the Doppler frequency (Hz), v_r is the radial velocity or the target (m/s), and λ is the transmitted wavelength (meters). The clutter spectral width in meters per second is independent of the radar frequency [Skolnik Ch. 15]. From equation 1.X the standard deviation of the power spectrum in velocity can be related to the standard deviation of the power spectrum in frequency as

$$\sigma_c = \frac{2\sigma_v}{\lambda} \tag{3.2}$$

where λ is the transmitted wavelength, is σ_c is standard deviation of clutter in Hz, and σ_v is standard deviation of clutter expressed in velocity [Skolnik Ch. 15].

To calculate the required clutter attention (CA) for the system, the average amplitude of background clutter due to the background must be calculated. The amplitude of the clutter signal is dependent on the size of the resolution cell of the radar, the frequency of the radar, and the reflectivity of the clutter [Skolnik Ch. 15]. The average radar cross section (RCS) of ground-based clutter, $\overline{\sigma}$, can be calculated as

$$\overline{\sigma} = A_c \sigma^0 = R\theta_{az} \frac{c\tau}{2} \sigma^0 \tag{3.3}$$

$$\overline{\sigma} = (55.56 * 10^3 m)(0.02182 rad) \frac{(3e8 m/s)(2 * 10^{-6} s)}{2}(0.01) \approx 3637 m^2 = 35.6 dB \tag{3.4}$$

From the calculation above in Equation 1.X, the RCS contribution from background clutter is much stronger than that from the signal. However, the detected signal magnitude should be 15dB larger than that of clutter for accurate detection, indicating that clutter attenuation will be required. Knowing the average RCS of background clutter contribution from the wooded hills, the required clutter attenuation (CA_{req}) can now be calculated as

$$\text{Required } (S/C)_{ratio} = 15\text{dB} \approx 31.63 = \sigma_{target} / \sigma_{clutter} \tag{3.5}$$

In dB: $CA_{req} = \sigma_{target} - \sigma_{clutter} - (S/C)_{dB} = 3\text{dBm}^2 - 35.6\text{dBm}^2 - 15\text{dB} = -47.6\text{dB}$

The level of clutter must be reduced by 47.6dB for accurate detection with this radar system. The figure listed in the project instructions has been successfully verified.

Objective B Simulation Results:

A Gaussian clutter spectrum was generated with a standard deviation of 2.79Hz relative to the PRF = 400Hz. The inverse FFT of the spectrum was taken to produce the Gaussian pulse in the time domain, seen in the Figure below. To generate the signal for simulation, this Gaussian pulse is added to a cosine function with a single frequency within the expected Doppler frequency range. This sum signal, called x[n], is fed through the pulse cancellers to produce an output called y[n].

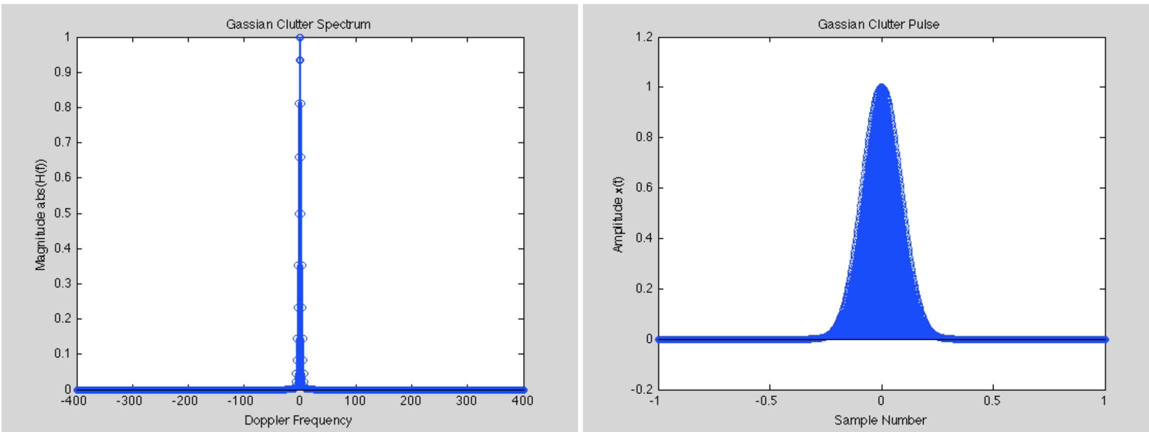

Figure 2: **Time and Frequency Response for Gaussian Clutter Spectrum**

*Units on x-axis have incorrect scaling. Should be in terms of sample number. Shape of plot is correct.

Two-Pulse Canceller (Gaussian Clutter 10dB Larger in Amplitude Than Signal):

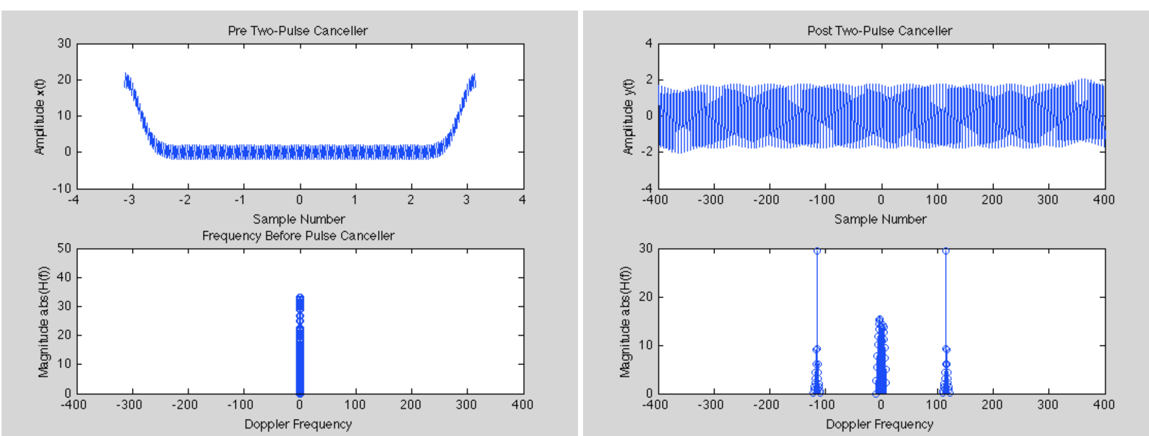

Figure 3: Frequency Response Before and After Appling Two-Pulse Canceller

Two-Pulse Canceller (Gaussian Clutter 32.6dB Larger in Amplitude Than Signal):

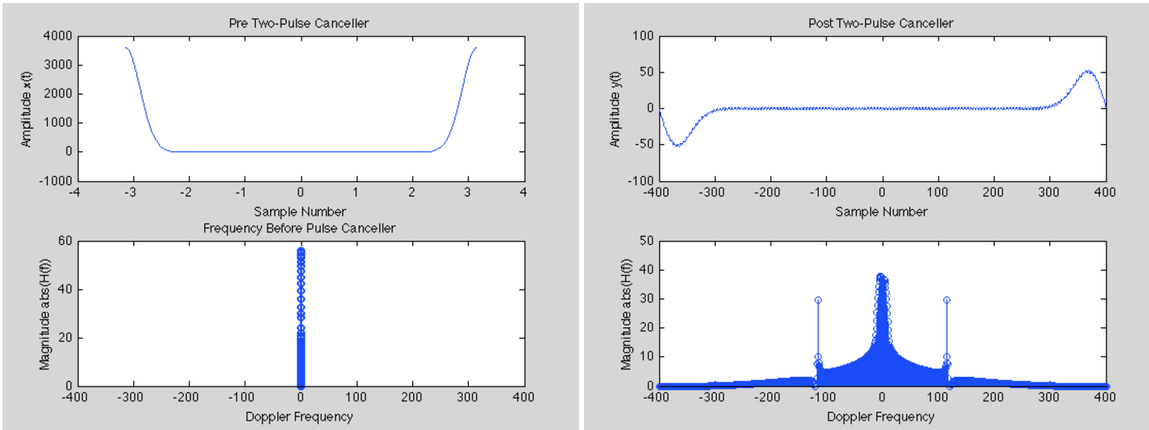

Figure 4: Frequency Response Before and After Appling Two-Pulse Canceller

Three-Pulse Canceller (Gaussian Clutter 32.6dB Larger in Amplitude Than Signal):

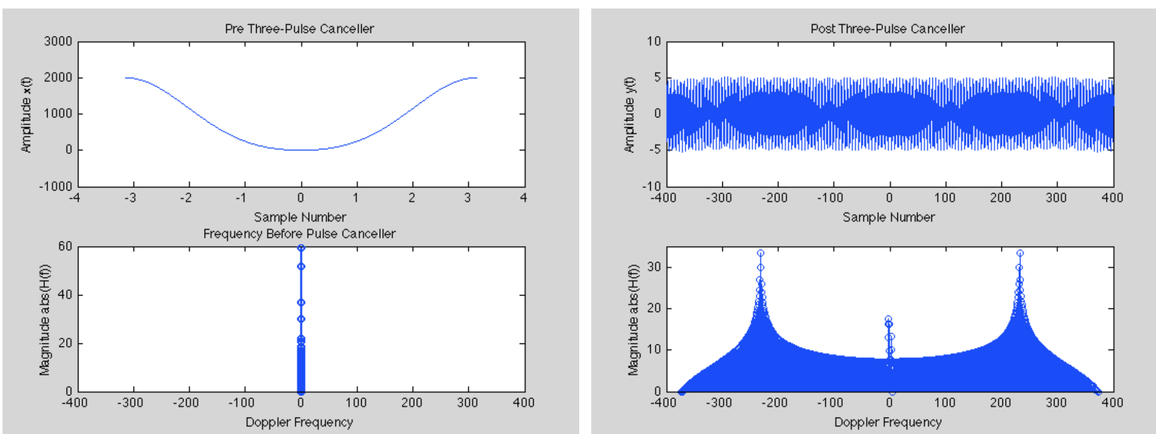

Figure 5: Frequency Response Before and After Appling Three-Pulse Canceller

It appears that the three-pulse canceller is giving nearly 15dB of margin between the between the received target Doppler frequency, modeled by a cosine, and the low-frequency clutter spectrum. The (S/C) is near 15dB making the three-pulse canceller a success.

Objective B: Design on a N-pulse Canceller for Clutter Suppression Using Minimum Number of Pulses

As stated in the introduction, N-pulse cancellers are typically implemented as low order, simple MTI filter designs used to attenuate stationary and very slow moving clutter. In this section, an N-pulse canceller must be designed to meet the 47.6dB clutter attenuation level determined in the previous section. The conventional two-pulse and three-pulse non-recursive FIR filters will be analyzed to see whether either meets the required system performance. As previously stated, the goal of MTI filtering is to reduce clutter. In this analysis, clutter attenuation (CA) and improvement factor (I) will be used as MTI figures of merit to evaluate the performance of the N-pulse cancellers.

The clutter attenuation can be defined as the ratio of clutter power at the input of the MTI filter to the clutter power at the output of the MTI filter as defined below

$$CA = \frac{\sigma_{ci}^2}{\sigma_{co}^2} \quad (3.6)$$

where σ_{ci}^2 and σ_{co}^2 = the clutter power at the filter input and output, respectively, as shown in *FRSP* Equation *5.43*.

The improvement factor, I, used in this analysis will be in the form [Levanon 1988]

$$I = \frac{(S/C)_{out}}{(S/C)_{in}}\left(\frac{S_{out}}{S_{in}}\right)\left(\frac{C_{in}}{C_{out}}\right) = (G)(CA) \qquad (3.7)$$

where G is the signal gain due to the filter. Generally, the it is assumed that the target velocity is unknown a priori and the average gain over all possible Doppler shifts is calculated as the signal gain [FRSP, pg. 246]. If the frequency response of the filter is known, it is easy to calculate the signal gain as

$$G = \frac{1}{PRF}\int_{-PRF/2}^{PRF/2} |H(F)|^2 \, dF \qquad (3.8)$$

To continue the derivation, refer to equations 5.50-5.52 in Richards *FRSP*. It was shown in Table 1.1 that the normalized standard deviation of clutter power in terms of angular frequency can be defined as σ_ω= (2π)(σ_f) = (2π)(6.98e-3) = 0.0438 rad/s. As stated by Richards in Equation 5.53 of FRSP, assuming σ_ω<< π, the normalized autocorrelation function for a Gaussian function can be approximated by

$$\rho_c[k] \approx e^{-(\sigma_\omega k)/2} \quad (3.9)$$

For the two-pulse canceller, the improvement factor can be defined as

$$I = CA*G = 1/(1 - \mathrm{Re}\{\rho_c[1]\}) = \frac{1}{1-e^{-\sigma_\omega^2/2}} = \frac{1}{1-e^{-(0.0438)^2/2}} \approx 1043 = 30.2\text{dB} \quad (3.10)$$

As stated as by Richards [FRSP pg. 247] and is easily calculated using Equation 3.8 above, *G* = 2 or 3dB, resulting in a *CA* = 27.2dB for the two-pulse canceller which does not meet the system requirements because it is *CA* < 47.6dB.

Next the conventional three-pulse canceller will be analyzed to see if it meets the system requirements for *CA*. As shown by Richards [FRSP pg. 247] in Equation 5.54,

$$I = CA*G = \frac{1}{1-(4/3)e^{-\sigma_\omega^2/2}+(1/3)e^{-2\sigma_\omega^2}} = \frac{1}{1-(4/3)e^{-(0.0438)^2/2}+(1/3)e^{-2(0.0438)^2}} \approx 543*10^3 = 57.3\text{dB} \quad (3.11)$$

For the three-pulse canceller, the signal gain can be calculated as

$$G = \frac{1}{400}\int_{-400/2}^{400/2}\left|4\sin^2\left(\frac{\pi F}{400}\right)\right|^2 dF = 6 = 7.8\text{dB}. \quad (3.12)$$

$$\text{In dB: } CA_{dB} = I_{dB} - G_{dB} = 57.3\text{dB} - 7.8\text{dB} = 49.5\text{dB} > 47.6\text{dB} = CA_{req} \quad (3.13)$$

From these results, it appears that the three-pulse canceller adequately meets the clutter attenuation for the three-pulse canceller. Since the two-pulse canceller did not meet the requirements, it will be determined that the three-pulse canceller uses the smallest number of pulses for a N-pulse canceller to meet the system requirements for clutter attenuation.

In addition, this analysis will argue that improvement factor is the figure of merit, which should be focused on in this section rather than clutter attenuation. This argument is made because improvement factor, defined as I = G*CA, accounts for both signal gain and clutter attenuation. Both of these factors directly correlate to the effective signal-to-clutter (S/C) ratio of the radar system and would be included in the traditional signal-to-noise (SNR) radar equation found in many texts. If the CA does not fulfill the (S/C) ratio, but the improvement factor does, the target will meet the (S/C) threshold and be accurately detected.

Objective C: Design Digital Filter Bank for Clutter Suppression Using Smallest Number of Phase Weights

The third objective of this report is to design a digital filter bank using the smallest number of phase weights that meets the requirements. In Objective B, a N-pulse canceller was used to suppress clutter in the received radar signal. In this section, a more sophisticated alternative will be used called Pulse Doppler Processing, which implements a Doppler filter bank consisting of matched filters implemented as discrete Fourier transform (DFTs). In Pulse Doppler Processing, the spectral analysis is performed by computing the DFT of the slow-time signal [Richards pg. 255]. The received signal of a target with a Doppler shift, FD, can be expressed in slow-time after quadrature demodulation as

$$y[m] = Ae^{j2\pi F_D mT};\ m = 0,\dots, M\text{-}1 \tag{3.14}$$

where M is the number of pulses over a single Dwell and T = 1/PRF.

If there is a large amount stationary or very low speed clutter, as we saw in the MTI case in Objective B, the received signal will have a very poor (S/C) ratio preventing detection of the Doppler shift target. As shown in Section 5.2.2 of FRSP on pg. 234, the signal-to-interfere (SIR) ratio can be maximized by implementing a matched filter.

The magic of Pulse Doppler Processing is that since the K-point DFT computes K different outputs from each input vector, it effectively implements a bank of K matched filters at once, each tuned to a different Doppler frequency [FRSP pg. 262]. As shown in Equation 5.90 of FRSP, the impulse response vector of the matched filters can be expressed as

$$\mathbf{h}_k = [1 \quad \exp(-j*2\pi k/K) \quad \exp(-j*4\pi k/K) \quad \ldots \quad \exp(-j*2\pi(K-1)*k/K)]' \qquad (3.15)$$

The corresponding discrete-time frequency response of this vector is

$$H_k(\omega) = \sum_{m=0}^{K-1} h_k[m]e^{-j\omega m} = \sum_{m=0}^{K-1}(1)e^{-j(\omega+2\pi k/K)m} \qquad (3.16)$$

The ability to implement the complicated matched filter bank with a simple DFT is great, however, major side lobes will still occur from the stationary and very low Doppler frequency clutter. As stated previously, these greatly diminish the (S/C) ratio. Assuming the standard rectangular window is applied, the peak side lobes will only be attenuate by 13dB. Given that clutter needs to be attenuated by *CA* = 47.6dB in this exercise, the standard rectangular window will not be adequate.

For best performance in clutter suppression, it is critical that the window function, such as a Hamming window, is applied before Doppler processing. Else the stationary and low frequency clutter will still distort the DFT prevent the target signal from being retrieved.

There are a number of common windowing functions used to dramatically decrease peak side lobe levels of a DFT sample. However, there is a trade-off that must be considered in choosing a windowing function. Generally, as side lobe suppression increases, the peak processing gain decreases, main lobe width increases, and SNR decreases. This is summarized in the table below.

Peak Side Lobes	Main lobe width	Peak Gain	SNR
↓	↑	↓	↓

Table 2: Summary of Tradeoffs Associated with Data Windowing Functions

In this analysis the standard rectangular window will be compared to the common Hamming window and the Blackman window. The characteristics will be summarized in the Table below. Some of the characteristics for the Blackman filter could not be easily located.

	Rectangular Window	Hamming Window	Blackman
Function	w[n] = 1	(See Below)	(See below)
Peak Side Lobe Level (dB)	-13	-43	-58.1dB
Main Lobe Width (relative to rect.)	1.0	1.46	
Peak Gain (dB) (relative to rect.)	0.0	-5.4	
SNR Loss (dB)	0.0	-1.35	

$$\text{Hamming Window: } w[n] = 0.54 - 0.46\cos(2\pi(n/N));\ 0 \le n \le N \tag{3.17}$$

$$\text{Blackman Window: } w[n] = 0.42 - 0.5\cos(2\pi(n/(N-1))) + 0.08\cos(4\pi(n/(N-1)));\ 0 \le n \le N \tag{3.18}$$

Objective C Simulation Results:

Standard Rectangular Window:

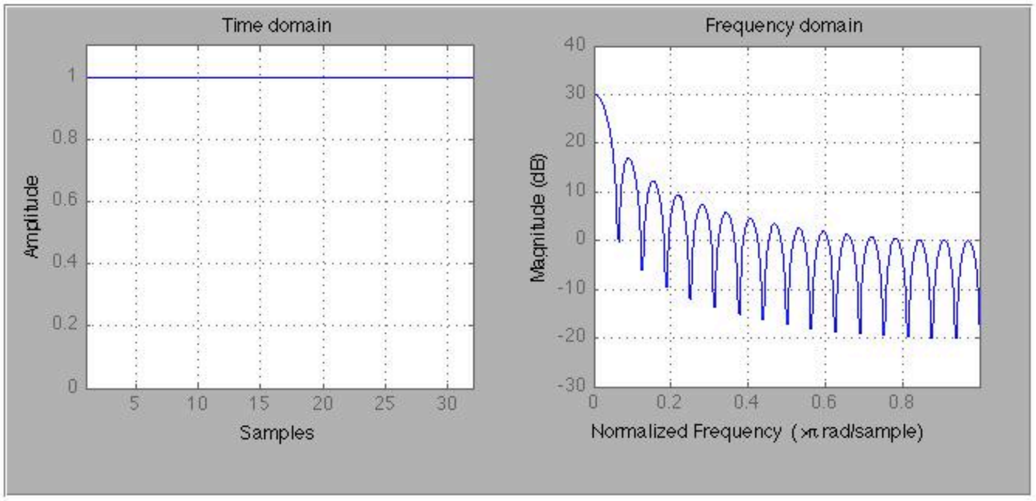

Figure 6: Time and Frequency Response of Standard Rectangular Window (N=32)

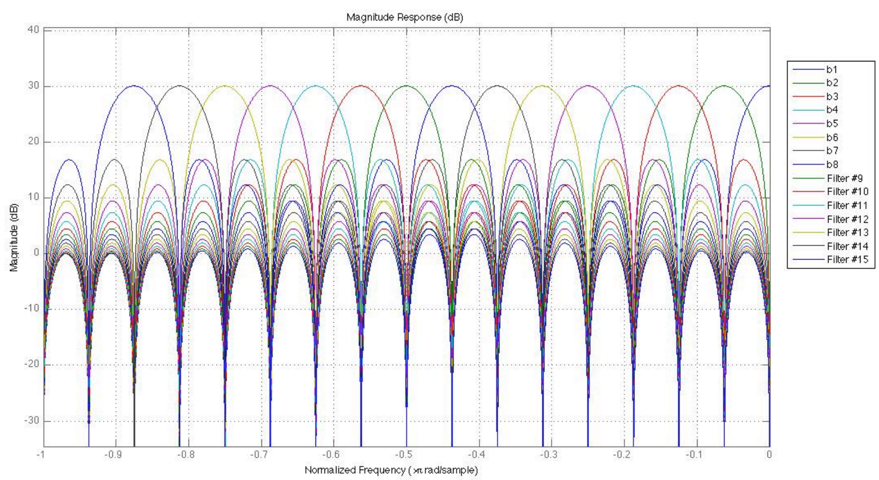

Figure 7: Negative Frequency Half of Doppler Filter Bank Using Rectangular Window (M = 30 filters, N=32 pulses)

Hamming Window:

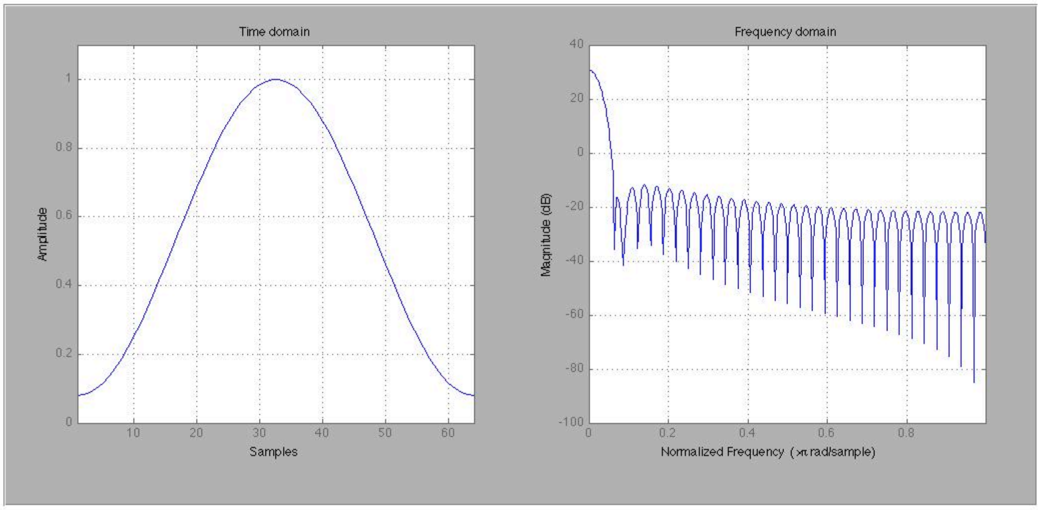

Figure 8: Time and Frequency Response of Hamming Window (N=32)

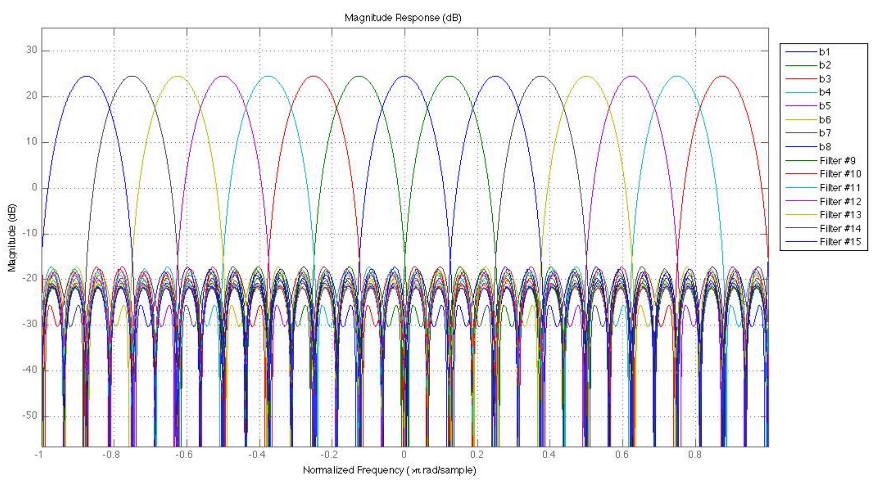

Figure 9: Hamming Window Filter Bank (M=15 filters, N=32pulses)

With PRF = 400, the normalized frequencies correlate to 0.125 rad/sample → 50 Hz and 0.875 rad/sample → 350 Hz. Given that targets above 350 Hz Doppler Shift are ignored by this radar, only 15 filters are used in this configuration to save one phase weight on the DFT. Technically, the center filter covering 0^o degrees is not relevant for this system. However, the stationary and low frequency clutter filter was not removed, because presence of stationary clutter, such as bad weather, may be of safety interest to the air traffic controllers. Also, if there are helicopters hovering stationary near the airport, they would be useful to detect.

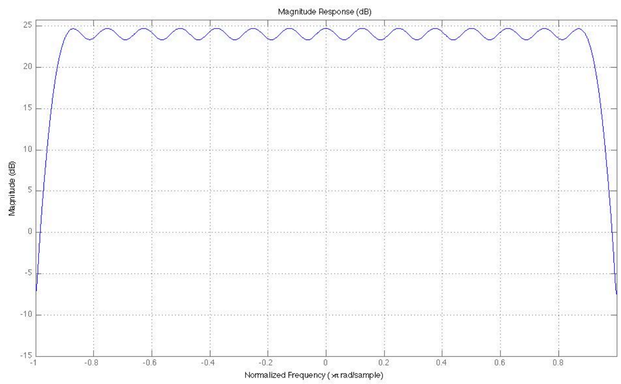

Figure 10: Summation of Filter Coefficients for All Filters in Hamming Filter Bank

Blackman Window:

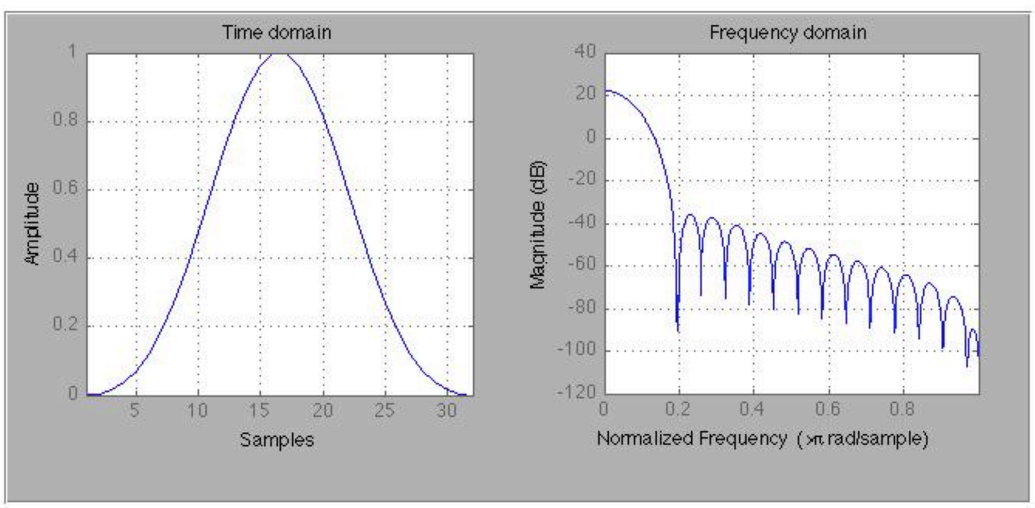

Figure 11: Time and Frequency Response of Hamming Window (N=32)

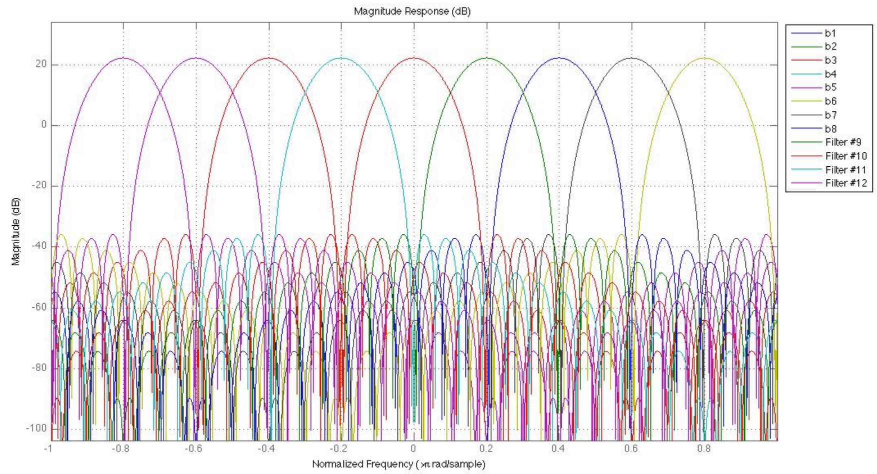

Figure 12: Hamming Window Filter Bank (M=9 filters, N=32pulses)

The Blackman filter shows by far the strongest performance, in terms of filter gain and side lobe levels, however, the cost is very wide main lobe. Most frequency regions have CA60dB and the worst nulls still have above CA50DB. For the two filters that overlap the center filter, covering stationary clutter, it is likely that ground clutter will cause many false alarms. However, this signal processing issue can probably be solved in software. Since the main lobes are so wide, it is likely that a received target signal may be detected by two different filter bins. Having a priori knowledge of the filter responses, the relative amplitudes at each filter receiving a response can be compared to make a fairly accurate estimate of the Doppler velocity.

As stated in the project report, the main lobe of the frequency response of the filter with $k = 1$ can be approximated by the function

$$H(f) = N*\sin[(N\pi f)/(2*PRF)] \quad (3.19)$$

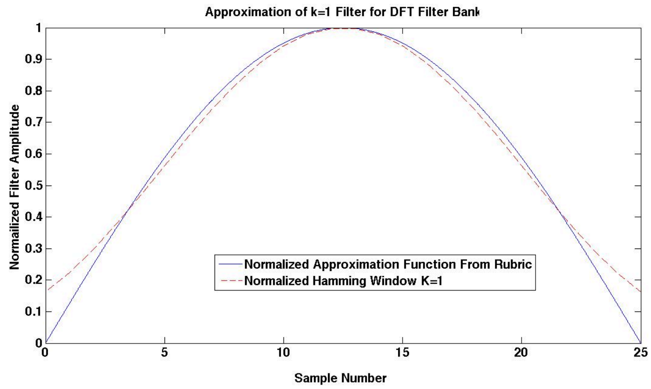

Figure 13: Approximation of k=1 Filter from DFT Filter Bank

IV.Conclusions

In this report, a method for calculating the amount of ground clutter for a wooded forest with a known reflectivity has been shown. More generally, this method extends to any type ground clutter detection given that its surface reflectivity is known and the illumination area of the system is known.

Further, the designs of two-pulse and three-pulse delay line cancellers were presented, the theoretical performance was calculated, and MATLAB simulation results were shown. For this system, the 3-pulse canceller is on the edge of meeting the specified requirements. The N-pulse delay line cancellers are great for reducing stationary or low-frequency clutter for a MTI radar system. However, the draw back for the N-pulse canceller MTI approach is that the system is plagued by blind spots at every multiple of the PRF limiting the unambiguous Doppler velocity calculation. It was not needed in this project, however, staggered multiple PRFs can be used to greatly increase the unambiguous range and Doppler velocity of a radar system. In future on the N-pulse canceller, the primary area of focus would be on attempting to improve performance by adding recursive feedback to the N-pulse cancellers to improve performance. If the radar engineer, wants a processing technique that is simple and easy to implement, than MTI using N-pulse cancellers may be the best choice.

With the advance in capabilities and decrease in cost of computers, high frequency electronics, and new signal processing techniques, more advanced methods than the MTI have been developed. The amount of computation and complexity of much higher, however, it is fair to say that computation is cheap. In the last section, it was shown that the complicated matched filter for optimal signal-to-interference ratio can be more simply implemented as a DFT filter bank. Using this method is known as Pulse Doppler Processing. In this method, we use a bank of filter to partially overlap and cover the desired frequency region for Doppler processing. The downside to this method, is the operator only know if there is a target in a given bin, but cannot distinguish the presence of multiple targets in the same bin. The other major drawback is the standard filters using a rectangular have high side lobe levels creating more false alarms. Side lobe levels can be reduced using windowing, but at the expense the expense of main lobe width and gain of the filters.

This study analyzed the rectangular window, the Hamming window, and the Blackman window. The Blackman window appears to be the strongest choice, however, additional signal processing will have to be done to reduce false alarm rates for the lowest frequency non-zero bins. The Hamming window is another popular and strong choice that seems to be close to meeting the system requirements. Depending on more specifics, the Hamming window may be a better choice in some situations.

In conclusion, different methods to calculate, analyze, and reduce stationary clutter and ground-based clutter were presented and simulated for use on an ARSR-3 civilian L-band radar system for commercial use. Using this signal processing capability to detect airborne target in the presence of large amounts of clutter is very important in keeping airport of the lives of pilots and passengers safe. As computational, hardware, and software capabilities continue to increase, more complex and more accurate methods will continue to be developed.

References

[1] Skolnik, M. I. (1970). Radar handbook. Chpater 15: MTI Radar

[2] Richards, M. A. Scheer, and Holm (2010). *Principles of modern radar: basic principles*. SciTech Pub.

[3] Levanon, N. (1988). Radar principles. *New York, Wiley-Interscience,*

[4] Richards, M. A. (2005). *Fundamentals of radar signal processing*. Tata McGraw-Hill Education.

[5] O'Donnell, R. M. (2009). Radar Systems Engineering Lecture 13 Clutter Rejection. IEEE New Hampshire